

**Dominant-negative regulation of cell surface expression by
a pentapeptide motif at the extreme COOH-terminal of a
Slo1 calcium-activated potassium channel splice variant**

YU-HSIN CHIU, CLAUDIA ALVAREZ-BARON, EUN YOUNG KIM, STUART E. DRYER*

Department of Biology and Biochemistry

University of Houston, Houston, TX 77204-5001, USA

Address Correspondence to: Dr. Stuart E. Dryer, Department of Biology and Biochemistry,

University of Houston, 4800 Calhoun, Houston, TX, 77204-5001, Tel 713-743-2697, FAX

713-473-2632, Email, SDryer@uh.edu

Running title: A carboxy-terminal trafficking motif in BK channels

Text pages 44

Figures 9

References 40

Words in Abstract 241

Words in Introduction 773

Words in Discussion 1472

Non-standard abbreviations

BK _{Ca} channels	Large-conductance Ca ²⁺ -activated K ⁺ channels
HA	hemagglutinin epitope
PI3 kinase	phosphoinositide-3 kinase
PDZ domain	PSD-95/Disks Large/Zonula Occludins (PDZ) domain
Slo1	Pore-forming subunit of BK _{Ca} channels

Abstract

Large conductance Ca^{2+} -activated K^+ (BK_{Ca}) channels regulate the physiology of many cell types. A single vertebrate gene variously known as *Slo1*, *KCa1.1*, or *KCNMA1* encodes the pore-forming subunits of BK_{Ca} channel, but is expressed in a potentially very large number of alternative splice variants. Two splice variants of Slo1, Slo1_{VEDEC} and Slo1_{QEERL}, which differ at the extreme COOH-terminus, show markedly different steady-state expression levels on the cell surface. Here we show that Slo1_{VEDEC} and Slo1_{QEERL} can reciprocally co-immunoprecipitate, indicating that they form heteromeric complexes. Moreover, co-expression of even small amounts of Slo1_{VEDEC} markedly reduces surface expression of Slo1_{QEERL} and total Slo1 as indicated by cell-surface biotinylation assays. The effects of Slo1_{VEDEC} on steady-state surface expression can be attributed primarily to the last five residues of the protein based on surface expression of motif-swapped constructs of Slo1 in HEK293T cells. In addition, the presence of the VEDEC motif at the COOH-terminus of Slo1 channels is sufficient to confer a dominant-negative effect on cell surface expression of itself or other types of Slo1 subunits. Treating cells with short peptides containing the VEDEC motif increased surface expression of Slo1_{VEDEC} channels transiently expressed in HEK293T cells, and increased current through endogenous BK_{Ca} channels in mouse podocytes. Slo1_{VEDEC} and Slo1_{QEERL} channels are removed from the HEK293T cell surface with similar kinetics and to a similar extent, which suggests that the inhibitory effect of the VEDEC motif is exerted primarily on forward trafficking into the plasma membrane.

Introduction

The pore-forming subunits of large-conductance Ca^{2+} -activated potassium (BK_{Ca}) channels are encoded by a conserved vertebrate gene called *Slo1* (also known as *KCNMA1* and *KCa1.1*) (Beisel et al., 2007). This gene encodes proteins with seven transmembrane domains (S0-S6), an ectofacial NH_2 -terminal, and a large intracellular COOH-terminus (Lu et al., 2006). A tetramer of Slo1 proteins can comprise a functional BK_{Ca} channel. The physiological importance of BK_{Ca} channels is underscored by the wide range of defects that occur when *Slo1* is knocked out (Meredith et al., 2004; Ruttiger et al., 2004; Sausbier et al., 2004) or after *in vivo* pharmacological blockade (Imlach et al., 2008).

The vertebrate *Slo1* gene has a conserved intron-exon structure, including at least 35 exons and no fewer than seven sites where alternative pre-mRNA splicing can occur (Beisel et al., 2007). The majority of alternative splice sites occur in the large cytosolic COOH-terminal domain, which comprises nearly half of each Slo1 subunit. Some of these variants have been analyzed and have been shown to encode channels with markedly different gating properties and susceptibility to posttranslational modulation (Butler et al., 1993; Tseng-Crank et al., 1994), such as the five Slo1 variants that differ at splice site 4 (Chen et al., 2005). Alternative splicing at site 7 as defined by Beisel et al. (2007) can result in three different extreme COOH terminal variants of Slo1 that are found across a wide range of vertebrate species. These include a long form known as Slo1_{VEDEC}, and two shorter forms known as Slo1_{EMVYR} and Slo1_{QEERL} (Ma et al., 2007; Kim et al., 2007b, 2007c, 2008)

after the last five residues in each isoform. Heterologous expression of these three COOH-terminal variants results in BK_{Ca} channels that have similar gating properties but markedly different patterns of expression on the cell surface (Ma et al., 2007; Kim et al., 2007b; Ridgway et al., 2009). All three of these variants contain an endoplasmic reticulum export signal described previously (Kwon and Guggino, 2004), whereas none of the ones studied contain a CVLF motif reported to suppress the surface expression of a subset of rat Slo1 splice variants (Zarei et al., 2004). Importantly, Slo1_{QEERL} and Slo1_{EMVYR} show much higher constitutive steady-state expression on the cell surface than Slo1_{VEDEC} (Kim et al., 2007b; Ma et al., 2007; Ridgway et al., 2009). However, the surface expression of Slo1_{VEDEC} approaches that of Slo1_{QEERL} and Slo1_{EMVYR} if cells are stimulated by appropriate growth factors (Kim et al., 2007b). In this study we focus on the Slo1_{VEDEC} and Slo1_{QEERL} variants because they have been shown to co-exist in different types of cells and tissues under normal conditions (Beisel et al., 2007; Kim et al., 2007b, 2008).

Previously, we demonstrated that the co-expression of a soluble fusion protein containing 42 of the unique COOH-terminal residues at the end of Slo1_{VEDEC} increased the surface expression of full-length Slo1_{VEDEC}, but had no effect on the surface expression of full-length Slo1_{QEERL} (Kim et al., 2007b). By contrast, co-expression of a fusion protein containing the unique COOH-terminal residues of Slo1_{QEERL} did not produce significant effects on the surface expression of either Slo1_{VEDEC} or Slo1_{QEERL} (Kim et al., 2007b).

These data suggest that a motif (or motifs) somewhere in the unique COOH-terminal tail of

Slo1_{VEDEC} can suppress constitutive surface expression of Slo1 proteins, but they provide no indication of where within the tail these motifs might be located. Ma et al. (2007) showed that progressive deletions of the unique portions of the Slo1_{VEDEC} COOH-terminal tail led to progressively greater surface expression of the remainder of Slo1_{VEDEC}. From this they concluded that the entire COOH-terminal tail of Slo1_{VEDEC} is important for its retention in intracellular compartments. However, this experimental design cannot exclude that progressive deletions cause increasingly severe disruptions of tertiary structure that affect Slo1 affinity for interactions with other proteins. In addition, deletions could cause motifs to be exposed that might normally be hidden in full-length proteins.

On the other hand, there is a substantial literature indicating that sequences as short as 4-5 residues at the extreme COOH-termini of proteins can contribute to functionally significant protein-protein interactions, especially interactions with PSD-95/Disks Large/Zonula Occludins (PDZ) domains. Consistent with this, we have recently reported that the Slo1_{VEDEC} isoforms can bind to proteins that do not interact with the other Slo1 splice variants (Kim et al., 2008) and that Slo1 proteins can interact with the PDZ domains of certain scaffolding proteins that regulate their trafficking (Ridgway et al., 2009). Based on these observations, we hypothesized that the differences in surface expression of Slo1 splice variants could reside in the last few residues of each variant. The purpose of the present study was to test this hypothesis.

Materials and Methods

Plasmid constructs

Expression plasmids encoding NH₂-terminal Myc-tagged Slo1_{VEDEC} and Slo1_{QEERL} variants of Slo1 were provided by Dr. Min Li of John Hopkins University (Kim et al., 2007b; Ma et al., 2007). These constructs are based on mouse sequences. Constructs encoding HA-tagged Short-QEERL and Short-VEDEC were obtained by PCR using Myc-tagged Slo1_{QEERL} as the template for the following paired primers:

5'-ATGGATGCGCTCATCATAACCGGTGACC-3'/5'-TGCGCCCGCTCAAAGCCGCTCTT
CCT-3' (Short-QEERL), and

5'-ATGGATGCGCTCATCATAACCGGTGACC-3'/5'-TCAACATTCATCTTCAACCACGTA
CTTCTG-3' (Short-VEDEC).

The constructs encoding Long-VEDEC and Long-QEERL were PCR amplified by using the Myc-tagged Slo1_{VEDEC} as a template with the following paired primers:

5'-GGTACCATGGATGCGCTCATCATAACCGGTG-3'/5'-TCAACATTCATCTTCAACTTC
TCTGATTG-3' (to produce Long-VEDEC), and

5'-GGTACCATGGATGCGCTCATCATAACCGGTG-3'/5'-TCAAAGCCGCTCTTCCTGTTC
TCTGATTGGAGG-3' (to produce Long-QEERL).

The PCR products were ligated into pCR2.1 (Invitrogen). After digestion of this plasmid with *KpnI* and *NotI*, the Slo1 variants were subcloned into pCMV-HA (Clontech). The

identity of these constructs was confirmed by sequencing.

Cell culture and transfection

Human embryonic kidney (HEK293T) cells were grown in Dulbecco's modified Eagle's medium (Invitrogen) containing heat-inactivated 10% fetal bovine serum (FBS) and penicillin-streptomycin (Invitrogen) at 37° in a 5% CO₂ incubator. Cells were transiently transfected for 24-48 hours using Lipofectamine2000™ (Invitrogen, CA) in serum-reduced medium (OPTI-MEM™, Invitrogen) following the manufacturer's instructions. An immortalized mouse podocyte cell line provided by Dr. Peter Mundel of the University of Miami was grown in RPMI1640 with 10% fetal bovine serum supplemented with 10 U/mL interferon- γ at 33° in a 5% CO₂ incubator. Differentiation of these cells was induced by removing interferon- γ and switching to 37° in a 5% CO₂ incubator for 14 days as described previously (Kim et al., 2008, 2009).

Cell-surface biotinylation, co-immunoprecipitation, and immunoblot analysis

Cell-surface biotinylation was carried out by labeling cells with 1 mg/mL EZ-Link Sulfo-NHS-Biotin™ reagent (Thermo Scientific) in PBS (137 mM NaCl, 10 mM NaPO₄, 2.7 mM KCl, pH 7.4) at 4° with gentle shaking for 1.5 hours. Labeled cells were then incubated in cold PBS containing 100 mM glycine for an additional 20 minutes at 4° to stop the reaction. Cells were lysed in PBS containing 0.5% Triton X-100 (Sigma-Aldrich) and a cocktail of

protease inhibitors (Sigma-Aldrich). Cell lysates were cleared by centrifugation and the supernatants were collected, and a portion of the supernatants was reserved for determination of the total expression of Slo1. The biotinylated proteins from the cell surface were recovered from the remainder of the lysates by incubating with immobilized streptavidin-agarose beads (Thermo Scientific) at 4° for 2 hours. Beads were washed in PBS and collected by centrifugation, and then boiled in 5X Laemmli buffer (50% glycerol, 10% SDS, 10% 2-mercaptaethonal, Tris 50 mM, 0.02% bromphenol blue).

For immunoprecipitation, cells were lysed and supernatants were collected as described above. Cell lysates containing 500 mg total proteins were incubated in the presence of mouse anti-Myc (9B11, Cell Signaling) or anti-HA antibodies (6E2, Cell Signaling) at 4°. After 4 hours of incubation, protein A/G agarose beads (Santa Cruz Biotechnology) were added to the lysates, which were kept at 4° for another 16 hours with gentle shaking. Beads were extensively washed in PBS, collected by centrifugation, and boiled in Laemmli buffer as described above. Samples were separated by 10 % SDS-PAGE and proteins were transferred to nitrocellulose paper followed by blocking in 5% nonfat dried milk dissolved in TBST buffer (10 mM Tris, 150 mM NaCl, and 0.1% Tween 20, pH 7.4). Slo1 proteins were detected by various primary antibodies, including mouse anti-Myc, mouse anti-HA, or rabbit anti-Slo1 (APC-107, Alomone Labs Ltd., Israel), as indicated. Horseradish peroxidase (HRP)-conjugated secondary antibodies (Cell Signaling) and SuperSignal West Pico

Chemiluminescent Substrate™ (Thermo Scientific) were used to visualize immunoreactive bands on autoradiography film. Results were scanned and processed by ImageJ software (distributed free of charge by NIH) to determine the intensities of signals.

Electrophysiology and data analysis

All recordings were made at room temperature (22°). Electrophysiological data were digitized and stored for off-line analysis using PClamp™ software (Molecular Devices). Whole-cell and inside-out patch recordings were performed in podocytes and HEK293T cells transiently expressing different Slo1 constructs using standard methods described in detail previously (Kim et al., 2007b, 2008, 2009; Zou et al., 2008). For whole-cell recordings from HEK293T cells, the bath solution contained 150 mM NaCl, 0.08 mM KCl, 0.8 mM MgCl₂, 5.4 mM CaCl₂, 10 mM glucose, 10 mM HEPES, and the pH was adjusted to 7.4 with NaOH. The pipette solution contained 145 mM NaCl, 2 mM KCl, 6.2 mM MgCl₂, 5 μM CaCl₂, 10 mM HEPES, and 5 mM *N*-(2-hydroxyethyl)ethylenediamine-*N*, *N*', *N*'-triacetic acid (HEDTA), pH 7.2. The free Ca²⁺ concentration in this solution was adjusted to 5 μM as determined using an Orion 97-20 calcium electrode (Thermo Fisher Scientific). Because HEK293T cells do not express endogenous voltage-activated Ca²⁺ channels, the pipette solution was designed to provide sufficient Ca²⁺ to activate BK_{Ca} channels, while the reduced K⁺ concentrations in bath and pipette salines ensured that macroscopic currents were small enough to avoid saturation of the patch-clamp amplifier. For measurements of whole-cell

currents conducted by endogenous BK_{Ca} channels in mouse podocytes, the bath solution contained 150 mM NaCl, 5.4 mM KCl, 0.8 mM MgCl₂, 5.4 mM CaCl₂, 10 mM HEPES, pH 7.4. Pipette solutions contained 10 mM NaCl, 125 mM KCl, 6.2 mM MgCl₂, 10 mM HEPES, pH 7.2, and 5 μM free Ca²⁺ buffered with 10 mM HEDTA, as determined with the calcium electrode. For whole cell recordings, currents were evoked by a series of depolarizing steps from a holding potential of -60 mV. For inside-out patch recordings of pseudo-macroscopic currents from HEK293T cells, fire-polished glass micropipettes were filled with a solution containing: 140 mM KCl, 1.2 mM MgCl₂, 14 mM glucose and 10 mM HEPES, pH 7.2, and had resistances of 2-5 MΩ after filling. Bath solutions contained: 140 mM KCl, 1.2 mM MgCl₂, 14 mM glucose, 10 mM HEPES, pH 7.2, and no added Ca²⁺ plus 10 mM EGTA, or 10 μM free Ca²⁺ buffered with 10 mM HEDTA. Currents were evoked by a series of 150-ms depolarizing steps from a holding potential of -80 mV. Activation curves were fitted to the Boltzmann function as described previously (Zou et al., 2008).

VEDEC peptide delivery

Penetratin-VEDEC and the octopeptide NH₂-IREVEDEC-COOH (IREVEDEC) were custom synthesized using a commercial service (Peptide 2.0 Inc., Chantilly, VA). Penetratin peptide (used as a control for Penetratin-VEDEC) was purchased from Innovagen (Lund, Sweden).

For cell surface biotinylation assays, HEK293T cells in 6-well tissue culture plates were transiently transfected with Slo1-containing plasmids as described above. After 30 hours of

incubation, transfected cells were washed with PBS and then incubated with a mixture of IREVEDEC and PULSin™ protein delivery reagent (Polyplus Transfection, Inc.) according to the manufacturer's instructions. This mixture was prepared by diluting 1 µg of IREVEDEC in 200 µL HEPES buffer pH 7.4 followed by addition of 12 µL PULSin™ reagent. This mixture was incubated at room temperature for 15 minutes and then added to transfected cells cultured in 2.8 mL DMEM per well. The same amount of R-phycoerythrin (R-PE) provided by the manufacturer was used with PULSin™ and added to a separate group of cells for use as a negative control. After 4 hours of incubation at 37°, the medium was replaced with regular culture media and cells were incubated for an additional 12 hours, at which point cell surface expression was assayed. To examine effects of VEDEC peptides on endogenously expressed BK_{Ca} channels, mouse podocytes were grown on coverslips coated with type I collagen. Peptide delivery was performed in two different ways. In the first, we prepared a mixture of 3 µg IREVEDEC or 3 µg R-PE in 100 µL HEPES and added 4 µL PULSin™ reagent, and then added this to cells cultured in 0.4 mL RPMI1640 medium. In separate experiments, podocytes were treated with 100 µM penetratin or penetratin-VEDEC in OPTI-MEM for 2-3 hours at 37°. Currents through BK_{Ca} channels were then measured using whole-cell recordings as described above.

Endocytosis assay

HEK293T cells were seeded at 30% confluence in 12-wells 24 hours before transfection.

Twenty-four hours after transfection, cells heterogeneously expressing Myc-tagged Slo1_{VEDEC} or Myc-tagged Slo1_{QEERL} were placed at 4° for 20 minutes to stop trafficking and degradation. Surface Slo1 was labeled with mouse anti-Myc in 4° medium for 1 hour. After an extensive wash with cold media, trafficking was allowed to resume by incubating cells at 37° for different periods of time. Cells were then fixed in PBS containing 4% paraformaldehyde without being permeablized. Anti-Myc remaining on the cell surface was detected using HRP-conjugated anti-mouse IgG and then exposed to *FAST* OPD™ reagents (Sigma-Aldrich) for 3 minutes with constant shaking, at which time the colorimetric reaction was stopped by adding 3 N HCl for 10 minutes at room temperature. The supernatant was collected and the optical absorbance was measured at 492 nm using a Multiskan MCC™ microplate reader (Fisher Scientific). The endocytosis time-constants (τ) were determined by fitting data to a first-order exponential decay function implemented in Origin™ software.

Immunocytochemistry and confocal microscopy

HEK293T cells heterologously co-expressing HA-tagged Slo1_{VEDEC} and Myc-tagged Slo1_{QEERL} were fixed in 4% paraformaldehyde in PBS at room temperature for 10 minutes. Fixed cells were permeablized and then blocked with PBS containing 0.5% Triton X-100 and 5% bovine serum albumin (BSA) at 37° for 1 hour. Cells were incubated in PBS containing rabbit anti-Myc (1:250, Upstate) and mouse anti-HA (1:250, Cell Signaling) with additions of 0.3% Triton X-100 and 3% BSA for 1 hour at 37°. After three washes in PBS, primary

antibodies were probed for 1 hour at 37° with Alexa Flour 568 conjugated anti-mouse IgG (1:1000, Molecular Probes) and AlexaFlour 488-conjugated anti-rabbit IgG (1:1000, Molecular Probes), which were diluted in PBS containing 0.3% Triton X-100 and 3% BSA. Cells were rinsed, mounted, and images were collected on an Olympus FV-1000 inverted stage confocal microscope using a Plan Apo N 60X 1.42NA oil-immersion objective, and processed by FluoView™ software.

Statistics

All quantitative data are presented as mean \pm S.E.M. Electrophysiological data were analyzed by Student's *t*-test with $P < 0.05$ considered as significant.

Results

Biochemical interactions between Slo1_{VEDEC} and Slo1_{QEERL}

Functional BK_{Ca} channels are minimally comprised of four Slo1 proteins, although auxiliary β -subunits can also be present in endogenously expressed channels. We have observed that the Slo1_{VEDEC} and Slo1_{QEERL} isoforms interact biochemically in a heterologous expression system. To do this, we transiently transfected HEK293T cells with plasmids that encode NH₂-terminal (ectofacial) HA-tagged Slo1_{QEERL} and Myc-tagged Slo1_{VEDEC}, and then carried out co-immunoprecipitations using antibodies against the tags. Using immunoblot analysis, we detected both HA and Myc when Slo1 was immunoprecipitated with either anti-Myc (Fig. 1A) or anti-HA (Fig. 1B). Neither tag was detected when the initial immunoprecipitation was carried out with normal mouse IgG. Consistent with these results, we observed partial co-localization of Slo1_{VEDEC} and Slo1_{QEERL} by confocal microscopy of transfected HEK293T cells using antibodies against the Myc and HA tags (Fig. 1C) suggesting that a substantial portion of the Slo1 proteins expressed under these conditions are heteromeric.

Co-expression of Slo1_{VEDEC} suppresses the steady-state surface expression of Slo1_{QEERL}

Previous studies have shown that Slo1_{QEERL} is normally expressed at relatively high levels on the cell surface, whereas Slo1_{VEDEC} is largely retained in intracellular pools (Kim et al., 2007b, 2007c, 2008, 2009; Ma et al., 2007). To examine the behavior of heteromeric channels, cell-surface biotinylation assays were carried out on HEK293T cells transiently expressing

HA-Slo1_{VEDEC} and Myc-Slo1_{QEERL} in different ratios (Fig. 2A). These assays were quantified by densitometry (Fig. 2B). In these experiments, the total amount of Slo1-encoding plasmid transfected into cells was the same in each group, which caused the total amount of Slo1 in the HEK293T cells to be constant as measured by immunoblot analysis of total cell lysates using anti-Slo1. While the total expression of Slo1 proteins remained the same in all groups of cells, the percentage that was on the cell surface was markedly decreased with even a modest increase of total Slo1_{VEDEC} expression relative to Slo1_{QEERL}. Thus, a 50% reduction in mean surface expression of Slo1 was observed when only 12.5% of the DNA transfected into the cells encoded Slo1_{VEDEC}, and 87.5% encoded Slo1_{QEERL} (Fig. 2B). These data suggest that Slo1_{VEDEC} has a dominant-negative effect on the steady-state expression of Slo1 proteins on the cell surface, probably by trapping heteromeric Slo1 proteins in intracellular compartments. Ma et al. (2007) reached a similar conclusion using a quantitative cell sorting procedure.

Motif-swapped constructs reveal a significant role for the last five residues of Slo1 splice variants

The wild-type Slo1_{VEDEC} and the wild-type Slo1_{QEERL} variants that we have studied are identical for their first 1108 residues. The Slo1_{QEERL} form has a short tail that extends 8 residues past the point where the two forms diverge, whereas Slo1_{VEDEC} has a long COOH-terminal tail that extends for 61 residues past the point where the isoforms diverge.

In principle, a signal that leads to retention of Slo1_{VEDEC} in intracellular compartments could lie anywhere within the 61-residue VEDEC tail, and Ma et al. (2007) suggested that the entire tail was involved based on deletions of progressively larger portions of the unique components in the Slo1_{VEDEC} tail. However, those sorts of deletions can produce distance effects on overall structure of the protein and can expose domains for interactions with other proteins that would not normally be available owing to steric constraints. Instead, we hypothesized that the essential portion would occur at the very end of the molecules, since with full length proteins these residues would be most likely to be exposed for interactions with other molecules. To test this hypothesis, we prepared constructs encoding a series of HA-tagged Slo1 proteins in which the last five residues were switched. These constructs are shown schematically in Fig. 3A, and include Slo1 channels with the long tail ending in VEDEC (the wild-type Slo1_{VEDEC}, hereafter called Long-VEDEC) and a motif-swapped version that is identical except that it ends in QEERL (hereafter called Long-QEERL). We also prepared Slo1 channels with short COOH-terminal tails that end in QEERL (the wild-type Slo1_{QEERL} form, hereafter referred to as Short-QEERL) and a switched version that ends in VEDEC (Short-VEDEC). All of these constructs are based on mouse sequences. We confirmed these constructs by sequencing, and were able to detect their transient expression in HEK293T cells by immunoblot analysis using either anti-HA or anti-Slo1 (Alomone APC-107) (Fig. 3B). This antibody did not produce any signal in non-transfected cells (data not shown). We then examined the cell-surface expression of these

COOH-terminal wild-type and motif-switched Slo1 variants by means of cell-surface biotinylation assays and whole-cell recordings in HEK293T cells (Figs. 4 and 5). Although Short-QEERL and Short-VEDEC showed similar levels of total expression, the surface expression of Short-VEDEC was markedly reduced compared to that of Short-QEERL (Fig. 4A, B), although non-linearities in cell surface biotinylation assays may result in underestimation of surface expression when signals are faint (Chae et al, 2005a). Consistent with this, the whole-cell current recorded from cells expressing Short-VEDEC was also significantly reduced compared to Short-QEERL (Fig. 4C), although the difference was not as pronounced. Note that in these recordings the recording electrodes contained a saline in which the free Ca^{2+} was buffered to 5 μM and currents were evoked by application of a series of depolarizing voltage steps. We also examined the effects of swapping VEDEC for QEERL at the end of the short Slo1 isoform using inside-out patches in the presence of 10 μM caused a modest right-shift in the voltage-dependence of activation at these voltages (Fig. 4D). However, this shift cannot account for the marked difference in currents measured at +60 mV, since channels with both COOH terminal motifs reach maximal activation at that potential. Therefore, the main effect of the motif swap was to change the density of Slo1 channels on the cell surface available for activation. Moreover, we observed a higher surface expression of Long-QEERL compared to Long-VEDEC (Fig. 5A, B) which was also reflected in qualitatively similar differences in whole-cell current (Fig. 5C). In inside out patches, we did not see any shift in the voltage-dependence of activation as a result of

swapping the terminal pentapeptide motif (Fig. 5D).

In another set of experiments, we examined whether the VEDEC motif can account for dominant-negative effects on Slo1 trafficking that we observed with co-expression of Slo1_{VEDEC}. Therefore, we transfected HEK293T cells with combinations of the Short-QEERL and Short-VEDEC constructs (which differ only in the last five residues) and examined surface expression of total Slo1 proteins using the approach already outlined in Fig. 2. We again observed that the presence of the VEDEC motif in only a small portion of the expressed proteins is sufficient to cause robust suppression of Slo1 expression on the cell surface (Fig. 6). These data strongly support the hypothesis that the VEDEC and/or QEERL motifs are involved in regulating the trafficking of Slo1 channels into or out of the cell surface.

VEDEC peptides promote the cell surface expression of Slo1

The data on swapped-motif constructs could be interpreted as a positive effect of the QEERL motif on surface expression, a negative effect of the VEDEC motif, or both. In this regard, we have previously shown that co-transfecting full-length Slo1_{VEDEC} channels with a fusion protein comprised of GFP and the last 42 residues from the COOH-terminus of Slo1_{VEDEC} increased the surface expression of full-length Slo1_{VEDEC} and increased whole-cell BK_{Ca} currents in HEK293T cells, whereas GFP alone was ineffective (Kim et al., 2007b). For this reason, we hypothesized that the VEDEC motif is sufficient to suppress cell surface

expression of Slo1 proteins. If this is the case, introducing short peptides containing the VEDEC motif into cells should also cause an increase in Slo1 expression on the cell surface (by competing with full-length channels for binding to an inhibitory site). In the present study we have used two different approaches to introduce these highly acidic peptides into the cytosol. In the first set of experiments, we synthesized the octopeptide IREVEDEC and delivered it into HEK293T cells expressing full-length Slo1_{VEDEC} or Slo1_{QEERL} using a commercially available proprietary reagent called PULSin™. A similar amount of R-phycoerythrin (R-PE) was introduced into control HEK293T cells (which also served to assess the efficiency of the peptide delivery system). We then examined the effect of these treatments on Slo1 using cell-surface biotinylation assays carried out in HEK293T cells heterologously expressing either Myc-Slo1_{VEDEC} or Myc-Slo1_{QEERL}. Delivery of IREVEDEC had no effect on the total expression of either Slo1 isoform (Fig. 7). However, the IREVEDEC octopeptide increased the surface expression of Slo1_{VEDEC} compared to that observed in the R-PE control (Fig. 7, A and B). By contrast, IREVEDEC treatment had no effect on the surface expression of Slo1_{QEERL} (Fig. 7, C and D). A similar effect of IREVEDEC was observed in a conditionally immortalized cell line derived from mouse podocytes that endogenously expresses Slo1_{VEDEC} and Slo1_{QEERL} (Kim et al., 2008). These experiments were carried out using whole-cell recordings, and the effect of IREVEDEC on podocyte BK_{Ca} currents was statistically significant (Fig. 8A). Moreover, we observed that IREVEDEC treatment did not alter the activation or deactivation kinetics of macroscopic

currents (data not shown). A similar result was obtained in podocytes using a different peptide in which the VEDEC motif was present at the end of the penetratin sequence (Fig. 8B). Penetratin is a 16-residue peptide derived from the third helix of the homeodomain of the Antennapedia protein of *Drosophila melanogaster* (Derossi et al., 1998; Derossi et al., 1994). As with several other arginine-rich peptides (Thoren et al., 2003), fusing the penetratin sequence to macromolecules allows them to be taken up by many cell types, although the mechanism whereby this occurs is not well understood. We had a 21-residue peptide synthesized that is comprised of the 16 penetratin residues and ending in VEDEC at the COOH-terminal (Pene-VEDEC). The 16-residue penetratin peptide (Pene) was used as a control. As with IREVEDEC, we observed that Pene-VEDEC was able to cause a statistically significant increase in whole-cell BK_{Ca} currents in podocytes compared to controls treated with Pene (Fig. 8B). These data support the hypothesis that the VEDEC motif binds to unknown proteins that anchor Slo1 proteins in intracellular compartments. As an aside we should note that treatment with Pene and Pene-VEDEC made the membranes of HEK293T cells somewhat fragile and difficult to patch.

Similar inward trafficking of Slo1^{VEDEC} and Slo1^{QEERL}

The steady-state surface expression of a membrane protein is determined by the rates and balance of movements into and out of the plasma membrane. While the presence of the VEDEC motif in Slo1 reduces constitutive steady-state expression on the cell surface, the

available data do not indicate how the VEDEC motif produces this effect. To examine this, HEK293T cells were transiently transfected with either Myc-Slo1_{QEERL} or Myc-Slo1_{VEDEC}. After 24 hr, the Slo1 proteins on the cell surface were labeled with mouse anti-Myc at 4 °C, and inward trafficking was then monitored by bring the cells back to 37°C for different periods of time. The anti-Myc antibodies remaining on the cell surface were labeled with HRP-conjugated anti-mouse IgG and quantified using a colorimetric assay that measured absorbance at 492 nm. In these experiments, the amounts of total expression of Slo1_{QEERL} and Slo1_{VEDEC} determined by immunoblot analysis were indistinguishable (data not shown). Based on this colorimetric assay, the total amount of Slo1_{QEERL} on the cell surface was greater than that of Slo1_{VEDEC} at the time at which cells are transferred back to 37° ($t = 0$), which is consistent with all other methods that we have used to analyze steady-state expression. Both Slo1 isoforms showed a subsequent exponential decline in cell surface expression over time that reached a new steady-state by 60 min, and the rate of internalization was indistinguishable for the two forms (Fig. 9). Specifically, the optical signal for Slo1_{VEDEC} declined with a time-constant of 14.4 ± 3.4 min and the steady-state decline of the signal (measured after 60 min) was 0.231 ± 0.065 optical density units (ODU₄₉₂). Signal for Slo1_{QEERL} declined with a time-constant of 15.1 ± 0.9 min and the steady-state decline after 60 min was 0.238 ± 0.037 ODU₄₉₂ (Fig. 9). These data suggest that the inward trafficking of both splice variants is carried out by similar mechanisms that have indistinguishable capacities and kinetics in HEK293T cells. These data suggest that the effects of the VEDEC

motif are exerted primarily on forward trafficking.

Discussion

In the present study, we have shown that two different COOH-terminal splice variants of Slo1, known as Slo1_{VEDEC} and Slo1_{QEERL}, are able to form heteromeric channels in a heterologous expression system. This is not surprising because both isoforms contain the tetramerization domain located between S6 and S7 identified previously (Quirk and Reinhart, 2001); indeed this domain is present in all Slo1 splice variants. Nevertheless, formation of this particular heteromeric complex has important functional consequences, as we have confirmed an earlier report (Ma et al., 2007) that Slo1_{VEDEC} can exert a dominant-negative effect on the steady-state expression of heteromeric channels to the cell surface, probably as a result of its binding to an as yet unidentified protein that traps the complex in intracellular compartments. This conclusion is supported by the observation that intracellular delivery of two small peptides that contain the VEDEC motif, IREVEDEC and Pene-VEDEC, is able to increase surface expression of heterologously and endogenously expressed Slo1 channels. It bears noting that the VEDEC motif is the only sequence element that these two small peptides have in common.

We and others have previously shown that Slo1_{QEERL} shows robust constitutive expression on the cell surface, whereas Slo1_{VEDEC} is preferentially maintained in intracellular compartments, at least until cells are stimulated with certain growth factors or in the presence of certain Slo1-interacting proteins (Kim et al., 2007a, 2007b). The present data attribute these differences in the behavior of the splice variants to small pentapeptide motifs at the

extreme COOH-termini of Slo1, a conclusion that is supported by examining the behavior of constructs in which only the last five residues are changed. Thus, Slo1 channels that end in the VEDEC motif have reduced surface expression regardless of whether they end in long or short COOH-terminal tails. While we cannot entirely exclude that the QEERL motif could play a positive role in cell-surface expression of Slo1, our earlier data suggest that this role is must be more limited than that of VEDEC. This is because co-expression of a fusion protein that contains the unique COOH-terminal domains of Slo1_{QEERL} did not produce consistent effects on steady-state surface expression of full-length Slo1, whereas a fusion protein that contained the COOH-terminal domains of Slo1_{VEDEC} behaved identically to the small peptides studied here (Kim et al., 2007b).

Ma et al. (2007) concluded earlier on the basis of sequential deletions of the unique portions of the Slo1_{VEDEC} tail that multiple domains were responsible for reduced surface expression of the Slo1_{VEDEC} isoform. While the present data cannot exclude that other COOH terminal motifs play a role in suppressing constitutive surface expression of this variant, they do suggest that the VEDEC motif can account for most of this effect.

Differences in experimental design can account for some of the difference in our interpretation; specifically, making substantial deletions can cause alterations in the structure of the entire COOH terminal such that interactions with other proteins could be altered. In addition, deletions could cause other motifs to become sterically available for interactions with other proteins, even though these motifs that may not normally be exposed or in a

position to interact in the wild-type forms of these channels. The present strategy of using swapped constructs and short peptide competitors that contain the VEDEC motif minimizes the difficulties in interpretation of results that arise with deletions.

The present study also provides evidence that Slo1_{QEERL} and Slo1_{VEDEC} are removed from the cell surface of HEK293T cells to a similar extent and by similar kinetics, at least over a period of one hour. The time course of Slo1 internalization is similar to that of other regulated surface proteins such as GLUT4, aquaporin, and glutamate receptors (Ehlers, 2000; Huang et al., 2001; Kamsteeg et al., 2006; Lin et al., 2000). Unfortunately, we have not been able to reliably measure the rate of forward trafficking under conditions where this process is kinetically isolated. However, by exclusion, our data suggest that the difference in the constitutive surface expression of Slo1_{VEDEC} and Slo1_{QEERL} is primarily due to differences in their rates of forward trafficking into the plasma membrane.

We have previously shown that Slo1_{VEDEC} and Slo1_{QEERL} are endogenously expressed in the same cell populations including chick ciliary ganglion neurons (Kim et al., 2007b) and mouse podocytes (Kim et al., 2008). In recent years, our group has examined the role of growth factor signaling cascades in regulation of the steady-state surface expression of Slo1 in chick ciliary ganglion neurons (reviewed in Dryer et al., 2003). In those cells, the surface expression of Slo1 is regulated by at least two different growth factors that signal through PI3 kinase cascades (Chae and Dryer, 2005; Chae et al., 2005a, b; Lhuillier and Dryer, 2002).

We have obtained preliminary data that suggest the presence of regulated trafficking of

endogenous Slo1 channels in podocytes as well (Kim, E. Y. and Dryer, S. E., unpublished observations). It seems likely that a similar type of regulation will occur in any cell type that expresses Slo1_{VEDEC}, regardless of which Slo1 variants may be co-expressed.

The mechanism whereby the VEDEC motif traps Slo1 in intracellular compartments is unknown. The VEDEC motif resembles type III PDZ-binding motifs, which are most typically found as the terminal sequence of proteins, and which have been shown to affect the trafficking and stability of other types of ion channels (Duggan et al., 2002; Maximov et al., 1999; Okabe et al., 1999; Standley et al., 2000). In this regard, we have recently reported that Slo1_{VEDEC} binds to one of the PDZ-domains of a scaffolding protein known as MAGI-1, which causes Slo1 to be sequestered in intracellular compartments in several cell types (Ridgway et al., 2009). While this would appear to be a promising candidate for a VEDEC-binding protein, we have also observed that MAGI-1 produces a similar effect on Slo1_{QEERL}, as well as on a third COOH-terminal variant known as Slo1_{EMVYR}, and can biochemically interact with all three COOH-terminal Slo1 variants (Ridgway et al., 2009). Thus, MAGI-1 is probably not responsible for the different trafficking behaviors of extreme COOH-terminal variants of Slo1 -- at least not by itself. The present results suggest a mechanism for Slo1_{VEDEC}-interacting proteins such as BK_{Ca} β -subunits (Kim et al., 2007c), filamin-A (Kim et al., 2007a), β 1 subunits of Na⁺-K⁺-ATPase (Jha and Dryer, 2009), and nephrin (Kim et al., 2008), which interact with the distal COOH-terminal and stimulate surface expression of Slo1_{VEDEC}. It is possible that interactions with these proteins sterically

inhibit access of the VEDEC motif to other proteins that suppress Slo1 expression on the cell surface. This would provide a basis for dynamic regulation of Slo1 expression based on protein interactions that change over time.

The observation that small VEDEC peptides can stimulate surface expression of Slo1 channels may be of pharmacological utility. Slo1 has received considerable interest as a target for therapies for a variety of neurological, cardiovascular, urological and pulmonary disorders (reviewed in Nardi and Olesen, 2008). The majority of drug development efforts to date have focused on modulator compounds that stimulate opening of BK_{Ca} channels that are already in the plasma membrane. The actions of the two short VEDEC peptides suggest a different strategy, namely to inhibit interactions between Slo1_{VEDEC} subunits and proteins that suppress their constitutive trafficking to the cell surface, thereby increasing the density of BK_{Ca} channel complexes at the cell surface. Our data in podocytes suggest that this can lead to an increase in the number of functional endogenously expressed BK_{Ca} channels at the cell surface. The fact that these compounds are short and very acidic peptides would normally be expected to reduce their usefulness as drugs for use *in vivo*, but because the essential motif is only five residues long, it might be possible to develop more stable and membrane-permeable analogs with a similar mode of action. It is also possible that agents of this type could increase surface BK_{Ca} channels at the expense of other compartments, e.g. mitochondria, where they may play a completely different physiological role. In this regard, we do not know the nature of the intracellular compartments that harbor Slo1_{VEDEC} subunits,

and it may well depend on what cell type is considered. In chick ciliary ganglion neurons, some of it may be associated with cortical actin in post-Golgi pools, at least in some cell types (Chae and Dryer, 2005; Chae et al., 2005b; Zou et al., 2008), whereas other pools are likely to be retained in the endoplasmic reticulum (Lhuillier and Dryer, 2002) and Golgi apparatus (Chae et al., 2005b).

In summary, we have shown that a pentapeptide motif at the extreme COOH-terminal of Slo1^{VEDEC} proteins is sufficient to impede constitutive trafficking of complexes containing this motif to the cell surface. Small peptides that contain this motif are able to stimulate expression of functional BK_{Ca} channels on the cell surface, and may suggest new pharmacological strategies for increasing BK_{Ca} function in cells.

Acknowledgments

We are grateful to Dr. Min Li of The Johns Hopkins University for the Myc-tagged Slo1 expression constructs, and to Dr. Peter Mundel of the University of Miami Miller School of Medicine for the immortalized podocyte cell line.

References

- Beisel KW, Rocha-Sanchez SM, Ziegenbein SJ, Morris KA, Kai C, Kawai J, Carninci P, Hayashizaki Y and Davis RL (2007) Diversity of Ca^{2+} -activated K^+ channel transcripts in inner ear hair cells. *Gene* **386**:11-23.
- Benkuský NA, Fergus DJ, Zuccherò TM and England SK (2000) Regulation of the Ca^{2+} -sensitive domains of the maxi-K channel in the mouse myometrium during gestation. *J Biol Chem* **275**:27712-27719.
- Butler A, Tsunoda S, McCobb DP, Wei A and Salkoff L (1993) mSlo, a complex mouse gene encoding "maxi" calcium-activated potassium channels. *Science* **261**:221-224.
- Chae KS and Dryer SE (2005) The p38 mitogen-activated protein kinase pathway negatively regulates Ca^{2+} -activated K^+ channel trafficking in developing parasympathetic neurons. *J Neurochem* **94**:367-379.
- Chae KS, Martin-Caraballo M, Anderson M and Dryer SE (2005a) Akt activation is necessary for growth factor-induced trafficking of functional K_{Ca} channels in developing parasympathetic neurons. *J Neurophysiol* **93**:1174-1182.
- Chae KS, Oh KS, and Dryer SE (2005b) Growth factors mobilize multiple pools of K_{Ca} channels in developing parasympathetic neurons: Role of ADP-ribosylation factors and related proteins. *J Neurophysiol* **94**:1597-605.
- Chen L, Tian L, MacDonald SH, McClafferty H, Hammond MS, Huibant JM, Ruth P, Knaus HG and Shipston MJ (2005) Functionally diverse complement of large conductance

calcium- and voltage-activated potassium channel (BK) alpha-subunits generated from a single site of splicing. *J Biol Chem* **280**:33599-609.

Derossi D, Chassaing G and Prochiantz A (1998) Trojan peptides: the penetratin system for intracellular delivery. *Trends Cell Biol* **8**:84-87.

Derossi D, Joliot AH, Chassaing G and Prochiantz A (1994) The third helix of the Antennapedia homeodomain translocates through biological membranes. *J Biol Chem* **269**:10444-10450.

Dhulipala PD and Kotlikoff MI (1999) Cloning and characterization of the promoters of the maxiK channel alpha and beta subunits. *Biochim Biophys Acta* **1444**:254-262.

Dryer SE, Lhuillier L, Cameron JS and Martin-Caraballo M (2003) Expression of K_{Ca} channels in identified populations of developing vertebrate neurons: role of neurotrophic factors and activity. *J Physiol Paris* **97**:49-58.

Duggan A, Garcia-Anoveros J and Corey DP (2002) The PDZ domain protein PICK1 and the sodium channel BNaC1 interact and localize at mechanosensory terminals of dorsal root ganglion neurons and dendrites of central neurons. *J Biol Chem* **277**:5203-5208.

Ehlers MD (2000) Reinsertion or degradation of AMPA receptors determined by activity-dependent endocytic sorting. *Neuron* **28**:511-525.

Huang J, Imamura T and Olefsky JM (2001) Insulin can regulate GLUT4 internalization by signaling to Rab5 and the motor protein dynein. *Proc Natl Acad Sci U S A* **98**:13084-13089.

- Imlach WL, Finch SC, Dunlop J, Meredith AL, Aldrich RW and Dalziel JE (2008) The molecular mechanism of "ryegrass staggers," a neurological disorder of K^+ channels. *J Pharmacol Exp Ther* **327**:657-664.
- Jha S and Dryer SE (2009) The $\beta 1$ subunit of Na^+/K^+ -ATPase interacts with BK_{Ca} channels and affects their steady-state expression on the cell surface. *FEBS Lett*.
- Kamsteeg EJ, Hendriks G, Boone M, Konings IB, Oorschot V, van der Sluijs P, Klumperman J and Deen PM (2006) Short-chain ubiquitination mediates the regulated endocytosis of the aquaporin-2 water channel. *Proc Natl Acad Sci U S A* **103**:18344-18349.
- Kim EY, Alvarez-Baron CP and Dryer SE (2009) Canonical transient receptor potential channel (TRPC)3 and TRPC6 associate with large-conductance Ca^{2+} -activated K^+ (BK_{Ca}) channels: role in BK_{Ca} trafficking to the surface of cultured podocytes. *Mol Pharmacol* **75**:466-477.
- Kim EY, Choi KJ and Dryer SE (2008) Nephtrin binds to the COOH terminus of a large-conductance Ca^{2+} -activated K^+ channel isoform and regulates its expression on the cell surface. *Am J Physiol Renal Physiol* **295**:F235-246.
- Kim EY, Ridgway LD and Dryer SE (2007a) Interactions with filamin A stimulate surface expression of large-conductance Ca^{2+} -activated K^+ channels in the absence of direct actin binding. *Mol Pharmacol* **72**:622-630.
- Kim EY, Ridgway LD, Zou S, Chiu YH and Dryer SE (2007b) Alternatively spliced C-terminal domains regulate the surface expression of large conductance

calcium-activated potassium channels. *Neuroscience* **146**:1652-1661.

Kim EY, Zou S, Ridgway LD and Dryer SE (2007c) Beta1-subunits increase surface expression of a large-conductance Ca^{2+} -activated K^+ channel isoform. *J Neurophysiol* **97**:3508-3516.

Kundu P, Alioua A, Stefani E and Toro L (2007) Regulation of mouse *Slo* gene expression: multiple promoters, transcription start sites, and genomic action of estrogen. *J Biol Chem* **282**:27478-27492.

Kwon SH and Guggino WB (2004) Multiple sequences in the C terminus of MaxiK channels are involved in expression, movement to the cell surface, and apical localization. *Proc Natl Acad Sci U S A* **101**:15237-15242.

Lhuillier L and Dryer SE (2002) Developmental regulation of neuronal K_{Ca} channels by $\text{TGF}\beta$ 1: an essential role for PI3 kinase signaling and membrane insertion. *J Neurophysiol* **88**:954-964.

Lin JW, Ju W, Foster K, Lee SH, Ahmadian G, Wyszynski M, Wang YT and Sheng M (2000) Distinct molecular mechanisms and divergent endocytotic pathways of AMPA receptor internalization. *Nat Neurosci* **3**:1282-1290.

Lu R, Alioua A, Kumar Y, Eghbali M, Stefani E and Toro L (2006) MaxiK channel partners: physiological impact. *J Physiol* **570**:65-72.

Ma D, Nakata T, Zhang G, Hoshi T, Li M and Shikano S (2007) Differential trafficking of carboxyl isoforms of Ca^{2+} -gated (Slo1) potassium channels. *FEBS Lett*

581:1000-1008.

- Maximov A, Sudhof TC and Bezprozvanny I (1999) Association of neuronal calcium channels with modular adaptor proteins. *J Biol Chem* **274**:24453-24456.
- Meredith AL, Thorneloe KS, Werner ME, Nelson MT and Aldrich RW (2004) Overactive bladder and incontinence in the absence of the BK large conductance Ca²⁺-activated K⁺ channel. *J Biol Chem* **279**:36746-36752.
- Nardi A and Olesen SP (2008) BK channel modulators: a comprehensive overview. *Curr Med Chem* **15**:1126-1146.
- Okabe S, Miwa A and Okado H (1999) Alternative splicing of the C-terminal domain regulates cell surface expression of the NMDA receptor NR1 subunit. *J Neurosci* **19**:7781-7792.
- Pietrzykowski AZ, Friesen RM, Martin GE, Puig SI, Nowak CL, Wynne PM, Siegelmann HT and Treisman SN (2008) Posttranscriptional regulation of BK channel splice variant stability by miR-9 underlies neuroadaptation to alcohol. *Neuron* **59**:274-287.
- Quirk JC and Reinhart PH (2001) Identification of a novel tetramerization domain in large conductance K(Ca) channels. *Neuron* **32**:13-23.
- Ridgway LD, Kim EY and Dryer SE (2009) MAGI-1 interacts with Slo1 channel proteins and suppresses Slo1 expression on the cell surface. *Am J Physiol Cell Physiol* **297**:C55-65.
- Ruttiger L, Sausbier M, Zimmermann U, Winter H, Braig C, Engel J, Knirsch M, Arntz C,

- Langer P, Hirt B, Muller M, Kopschall I, Pfister M, Munkner S, Rohbock K, Pfaff I, Rusch A, Ruth P and Knipper M (2004) Deletion of the Ca^{2+} -activated potassium (BK) alpha-subunit but not the BK beta1-subunit leads to progressive hearing loss. *Proc Natl Acad Sci U S A* **101**:12922-12927.
- Sausbier M, Hu H, Arntz C, Feil S, Kamm S, Adelsberger H, Sausbier U, Sailer CA, Feil R, Hofmann F, Korth M, Shipston MJ, Knaus HG, Wolfer DP, Pedroarena CM, Storm JF and Ruth P (2004) Cerebellar ataxia and Purkinje cell dysfunction caused by Ca^{2+} -activated K^+ channel deficiency. *Proc Natl Acad Sci U S A* **101**:9474-9478.
- Shen KZ, Lagrutta A, Davies NW, Standen NB, Adelman JP and North RA (1994) Tetraethylammonium block of Slowpoke calcium-activated potassium channels expressed in *Xenopus* oocytes: evidence for tetrameric channel formation. *Pflugers Arch* **426**:440-445.
- Shipston MJ (2001) Alternative splicing of potassium channels: a dynamic switch of cellular excitability. *Trends Cell Biol* **11**:353-358.
- Standley S, Roche KW, McCallum J, Sans N and Wenthold RJ (2000) PDZ domain suppression of an ER retention signal in NMDA receptor NR1 splice variants. *Neuron* **28**:887-898.
- Thoren PE, Persson D, Isakson P, Goksor M, Onfelt A and Norden B (2003) Uptake of analogs of penetratin, Tat(48-60) and oligoarginine in live cells. *Biochem Biophys Res Commun* **307**:100-107.

- Tseng-Crank J, Foster CD, Krause JD, Mertz R, Godinot N, DiChiara TJ and Reinhart PH
(1994) Cloning, expression, and distribution of functionally distinct Ca^{2+} -activated K^+
channel isoforms from human brain. *Neuron* **13**:1315-1330.
- Wang SX, Ikeda M and Guggino WB (2003) The cytoplasmic tail of large conductance,
voltage- and Ca^{2+} -activated K^+ (MaxiK) channel is necessary for its cell surface
expression. *J Biol Chem* **278**:2713-2722.
- Xie J and McCobb DP (1998) Control of alternative splicing of potassium channels by stress
hormones. *Science* **280**:443-446.
- Zarei MM, Eghbali M, Alioua A, Song M, Knaus HG, Stefani E and Toro L (2004) An
endoplasmic reticulum trafficking signal prevents surface expression of a voltage- and
 Ca^{2+} -activated K^+ channel splice variant. *Proc Natl Acad Sci U S A* **101**:10072-10077.
- Zarei MM, Zhu N, Alioua A, Eghbali M, Stefani E and Toro L (2001) A novel MaxiK splice
variant exhibits dominant-negative properties for surface expression. *J Biol Chem*
276:16232-16239.
- Zou S, Jha S, Kim EY and Dryer SE (2008). A novel actin-binding domain on Slo1
calcium-activated potassium channels is necessary for their expression in the plasma
membrane. *Mol Pharmacol* **73**:359-68.

Footnotes

This work was supported by the National Institutes of Health National Institute of Diabetes and Digestive and Kidney Diseases [Grant RO1-DK82529 to SED]

Address Correspondence to: Dr. Stuart E. Dryer, Department of Biology and Biochemistry,
University of Houston, 4800 Calhoun, Houston, TX, 77204-5001, Tel 713-743-2697, FAX
713-473-2632, Email, SDryer@uh.edu

Figure Legends

Figure 1. Co-immunoprecipitation and co-localization of Slo1_{VEDEC} and Slo1_{QEERL} in HEK293T cells.

Lysates of HEK293T cells heterologously expressing Myc-tagged Slo1_{VEDEC} and HA-tagged Slo1_{QEERL} were immunoprecipitated with either mouse anti-Myc (A) or anti-HA antibodies (B). Normal mouse IgG served as a negative control. The immunoprecipitated Slo1 proteins were detected with anti-HA or anti-Myc as indicated. C, co-localization of HA-tagged Slo1_{VEDEC} and Myc-tagged Slo1_{QEERL} in HEK293T cells visualized by confocal microscopy. Slo1_{VEDEC} was detected with anti-HA (green, a and b) and Slo1_{QEERL} was detected with anti-Myc (red, c and d). Merged signals of Slo1_{VEDEC} and Slo1_{QEERL} are shown in e-h. Boxed regions in e and f are magnified in g and h, respectively. Co-localization in merged images appear as a yellow signal.

Figure 2. Co-expression of Slo1_{VEDEC} reduces the surface Slo1_{QEERL} and Slo1 in a dose-dependent manner.

HEK293T cells were transiently co-transfected with Myc-tagged Slo1_{QEERL} and HA-tagged Slo1_{VEDEC}. The amounts of plasmids used are shown on the figures (in μg). A, results from representative cell-surface biotinylation assays. B, the total and surface expressions of Slo1 were quantified by densitometry and plotted as mean \pm S.E.M. of three experiments.

Figure 3. Motif-swapped constructs of Slo1.

A, schematic drawing of motif-swapped Slo1 constructs (not to scale). From the top to the bottom: Long-VEDEC, Long-QEERL, Short-QEERL, and Short-VEDEC. All of the constructs encode channels with an HA-tag at the NH₂-termini. White boxes represent the identical amino acid sequences in all Slo1 constructs. Gray boxes indicate the VEDEC-specific regions, and the black boxes indicate the QEERL-specific regions. The last five amino acids swapped are shown by letters. B, expression of motif-swapped Slo1 constructs after transient transfection of HEK293T cells determined by immunoblot analysis using the antibodies indicated.

Figure 4. Short-VEDEC has lower steady-state surface expression than Short-QEERL.

A, representative cell-surface biotinylation assays performed in HEK293T cells heterologously expressing Short-QEERL or Short-VEDEC, as indicated. Upper panel shows cell surface Slo1 while the lower panel shows expression of total Slo1. Signals were obtained by immunoblot analysis using antibodies against the Myc tags. B, summary of densitometric analysis of surface and total expression of Slo1 presented as mean \pm S.E.M. from three repetitions of the experiment in A. Upper plot shows normalized surface Slo1 whereas lower plot shows total expression of Slo1. C, representative traces of families of currents obtained by whole-cell recording from HEK293T cells expressing Short-QEERL or

Short-VEDEC are shown to the right of a bar graph summarizing mean \pm S.E.M. of whole-cell current densities evoked by step pulses to +60 mV (n = 34 cells). Asterisk indicates $P < 0.05$. D, voltage-dependence of activation determined in inside-out patches from HEK293T cells expressing Short-QEERL or Short-VEDEC. Recordings were made in symmetrical 140 mM KCl, and bath solutions contained 10 μ M free Ca^{2+} . Representative traces are shown above voltage activation curves. Data points are mean \pm S.E.M. (n = 11 patches) with superimposed fitted Boltzmann curves. Mean $V_{1/2}$ derived from the Boltzmann fits are -14.3 mV for Short-QEERL and +2.6 mV for Short-VEDEC.

Figure 5. Long-QEERL has higher surface expression than Long-VEDEC.

A, representative cell-surface biotinylation assays performed in HEK293T cells heterologously expressing Long-VEDEC or Long-QEERL, as in the previous figure. B, summary of densitometric analysis of surface and total expression of Slo1 presented as mean \pm S.E.M. from three repetitions of the experiment in A. C, representative traces of families of currents obtained by whole-cell recording are shown to the right of a bar graph summarizing mean \pm S.E.M. of whole-cell current densities evoked by step pulses to +60 mV (n = 34 cells). Asterisk indicates $P < 0.05$. D, voltage-dependence of activation determined in inside-out patches from HEK293T cells expressing Long-VEDEC or Long-QEERL. Recordings and voltage activation curves were made from 11 patches, as in the previous figure. Mean $V_{1/2}$ derived from the Boltzmann fits are -14.8 mV for

Long-QEERL and -20.1 mV for Long-VEDEC.

Figure 6. The VEDEC motif is sufficient to prevent Slo1 from being expressed on the cell surface.

HEK293T cells were transiently co-transfected with Myc-tagged Short-QEERL and HA-tagged Short-VEDEC. The amounts of plasmids used are indicated on the figures (in μg). A, results from representative cell-surface biotinylation assays, as well as analyses of total expression of the HA and Myc tags, as indicated. Note that total expression of each splice variant is closely related to the amount of each plasmid used in transfection. B, quantification (mean \pm S.E.M.) of densitometric analyses of three repetitions of this experiment. Note reduction of surface expression of Slo1 when even small amounts of Short-VEDEC are present.

Figure 7. IREVEDEC peptides increase the surface expression of Slo1_{VEDEC} in HEK293T cells.

In these experiments, 1 μg R-PE (Ctrl) or IREVEDEC peptide was delivered into HEK293T cells transiently expressing Slo1_{VEDEC} or Slo1_{QEERL} using PULSinTM reagent and cell-surface biotinylation assays were performed 12 hours later. Surface and total Slo1_{VEDEC} and Slo1_{QEERL} were detected with anti-Slo1 antibodies. A and C show results from representative cell-surface biotinylation assays. B and D show surface (upper panel) and

total (lower panel) expression of Slo1 quantified by densitometry and plotted as mean \pm S.E.M. from three different experiments compared to R-PE controls.

Figure 8. IREVEDEC and Penetratin-VEDEC peptides increase whole-cell currents in mouse podocytes.

Whole-cell recordings were made from differentiated mouse podocytes treated with R-PE or IREVEDEC peptide using PULSinTM (A), or podocytes treated with penetratin, or penetratin-VEDEC peptides (B). The recording electrode contained 5 μ M free Ca²⁺ and currents were evoked by a series of depolarizing steps from a holding potential of -60 mV. A, top panel shows representative whole-cell currents. Bar graph below shows mean \pm S.E.M. of whole-cell currents at +60 mV with $n = 33$ cells in each group (for IREVEDEC peptides), and 11 cells in each group for penetratin experiments. Asterisk indicates $P < 0.05$.

Figure 9. Time course of Slo1_{VEDEC} and Slo1_{QEERL} removal from the cell surface.

Endocytosis assays were carried out by using HEK293T cells heterologously expressing either Slo1_{VEDEC} or Slo1_{QEERL}. The expressed channels bear a Myc tag at the extracellular NH₂-terminus, which allowed surface Slo1 on the surface of intact cells to be labeled by anti-Myc at 4°. Cells were then placed at 37° for various times to allow trafficking to resume, at which time they were fixed. The amounts of anti-Myc remaining on the cell surface were determined by HRP-conjugated anti-mouse with colorimetric assays at OD492. Data show

the time course of OD492 (Mean \pm S.E.M.) from three different experiments. Filled squares indicate $Slo1_{VEDEC}$ and filled circles indicate $Slo1_{QEERL}$. Data are fitted with single-exponential decay functions with time constants of 15.1 ± 0.9 min (for $Slo1_{QEERL}$) and 14.4 ± 3.4 min (for $Slo1_{VEDEC}$).

Fig. 1

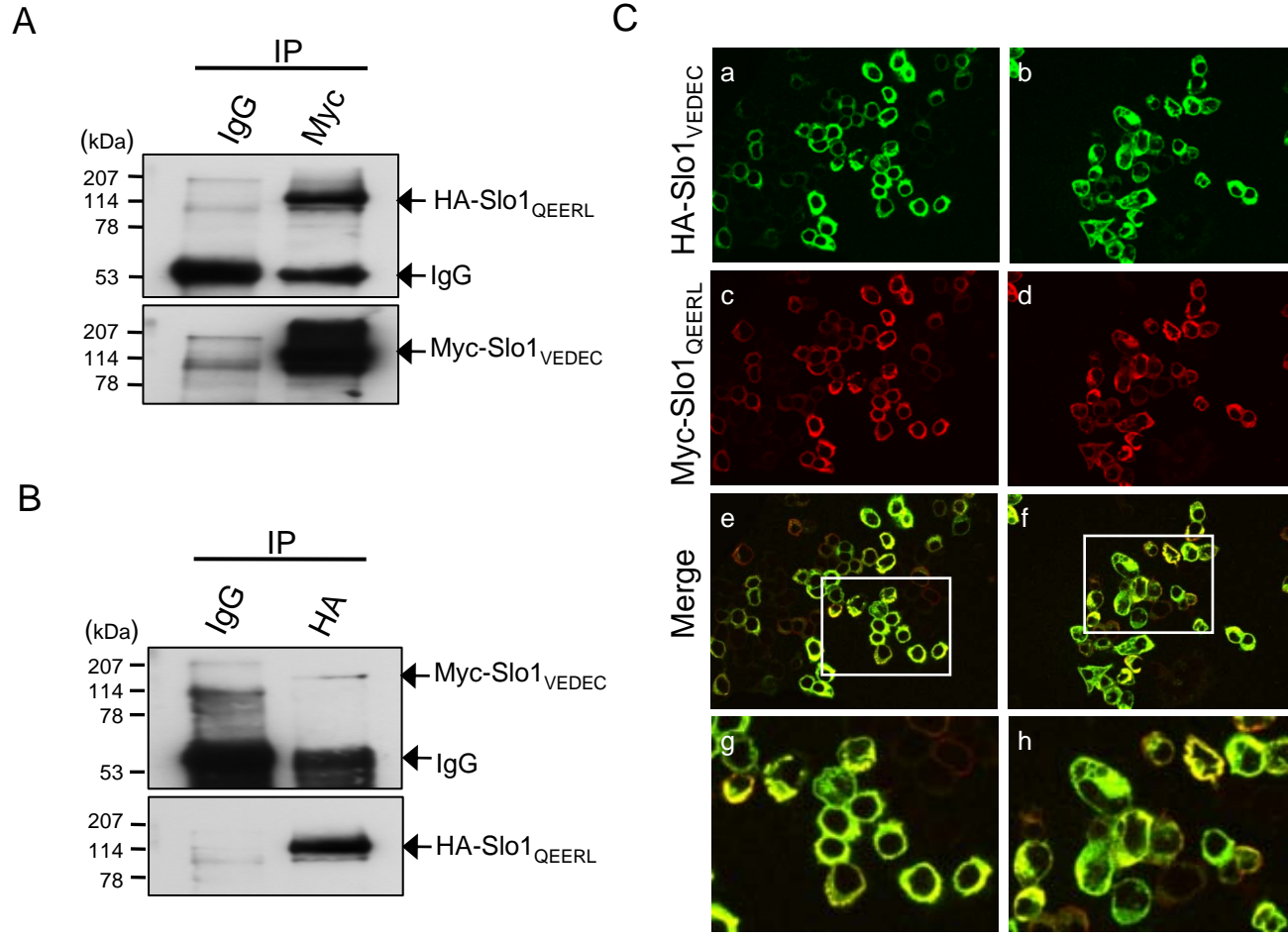


Fig. 2

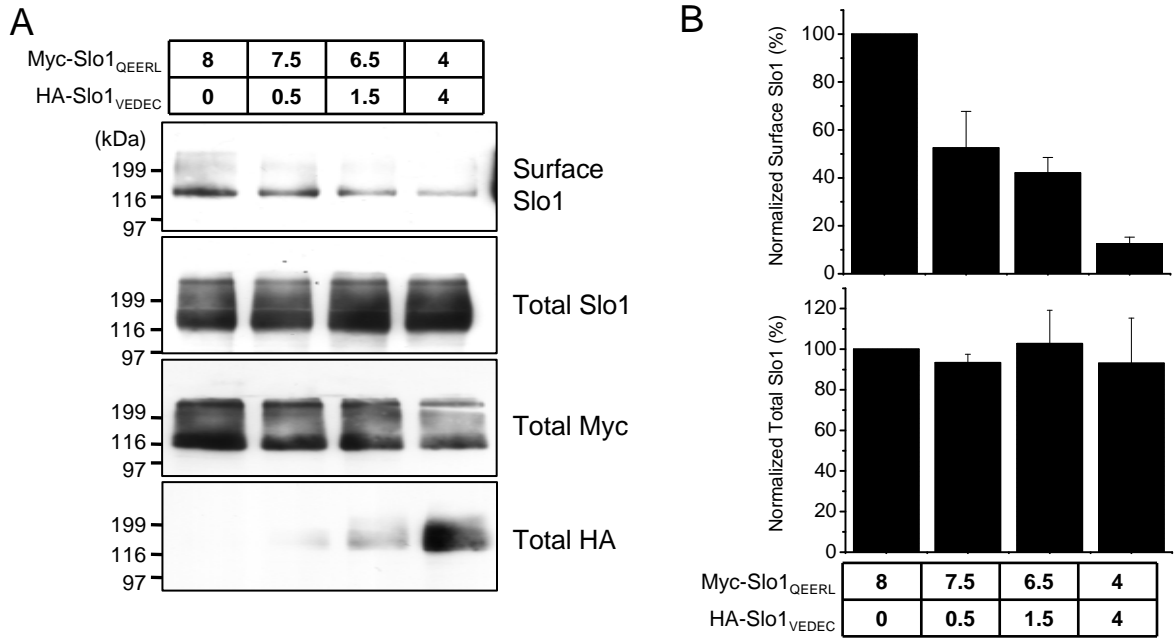


Fig. 3

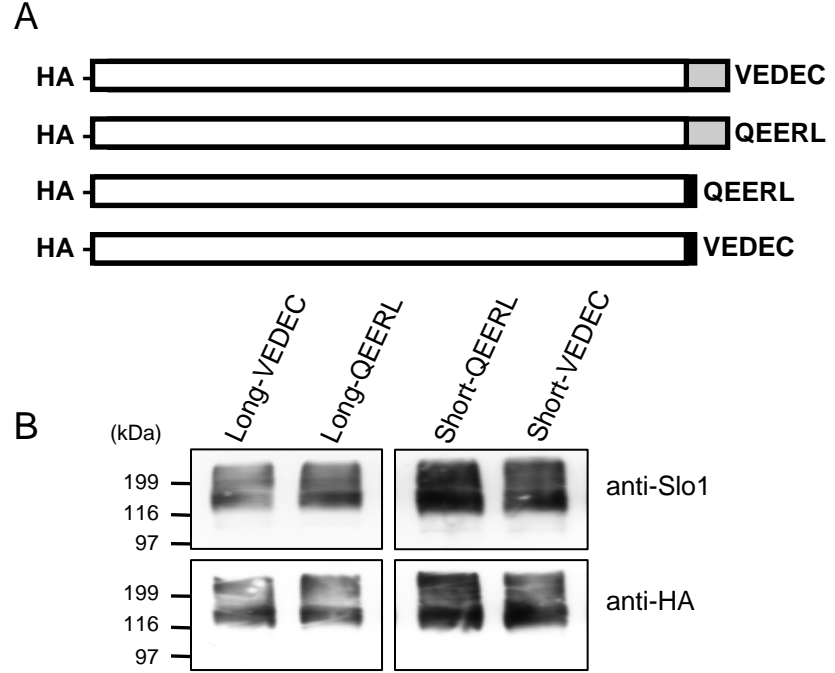


Fig. 4

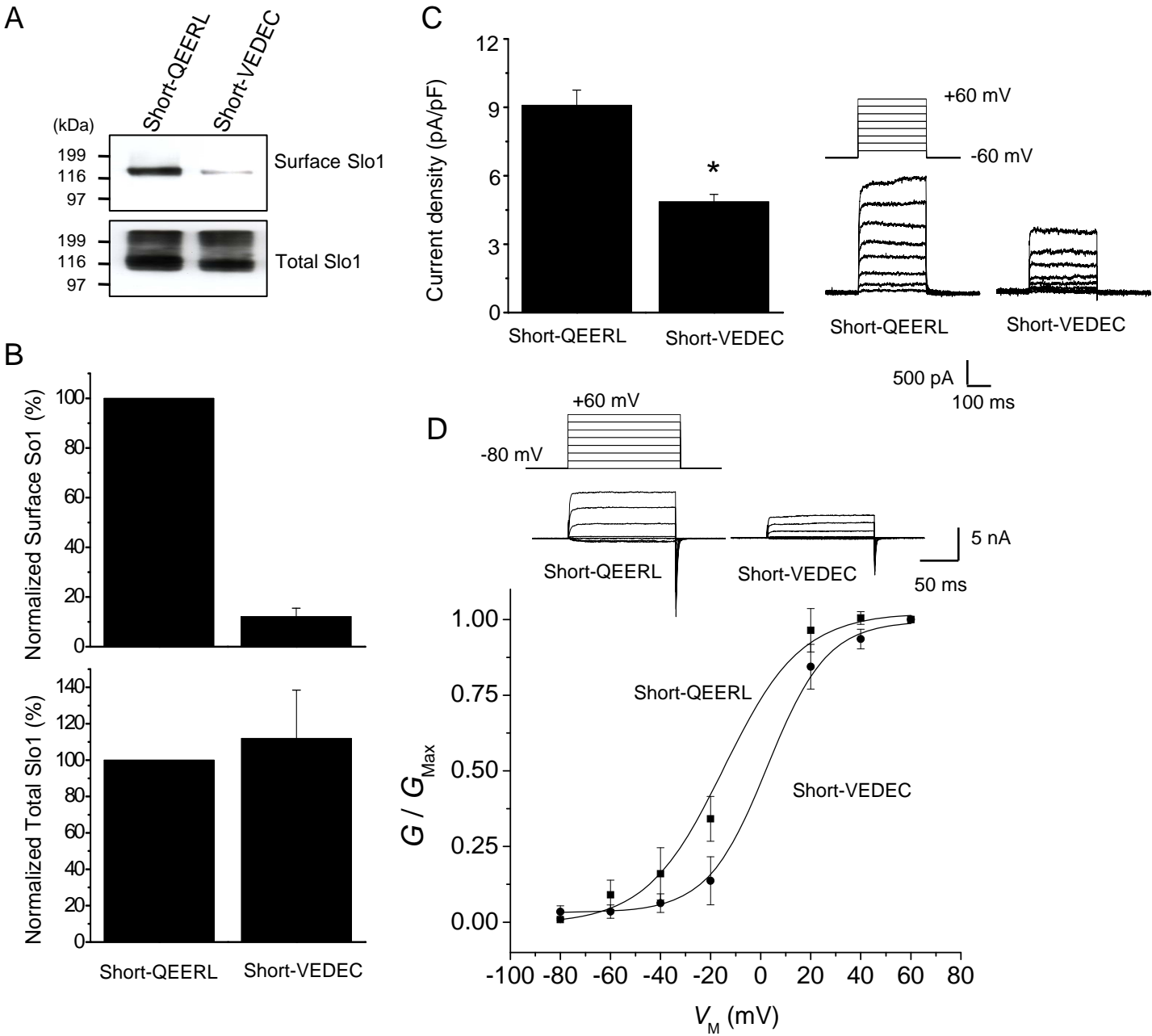


Fig. 5

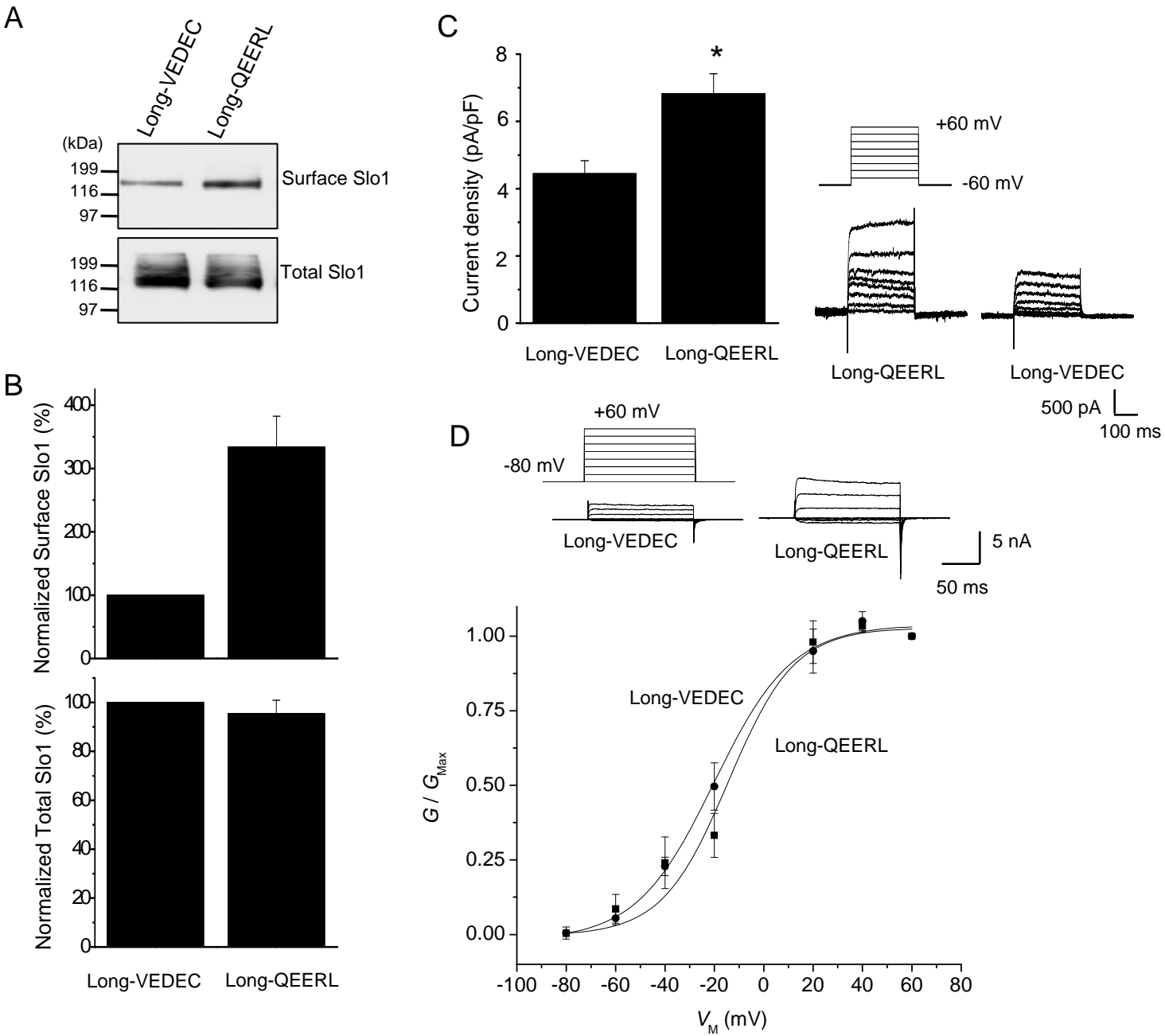
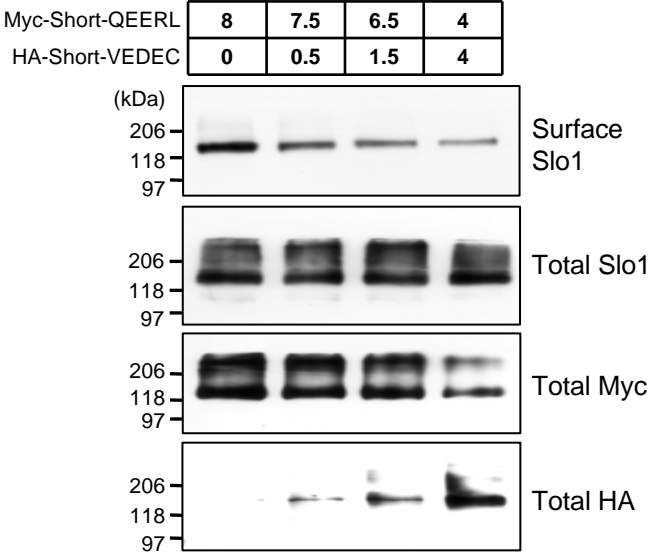


Fig. 6

A



B

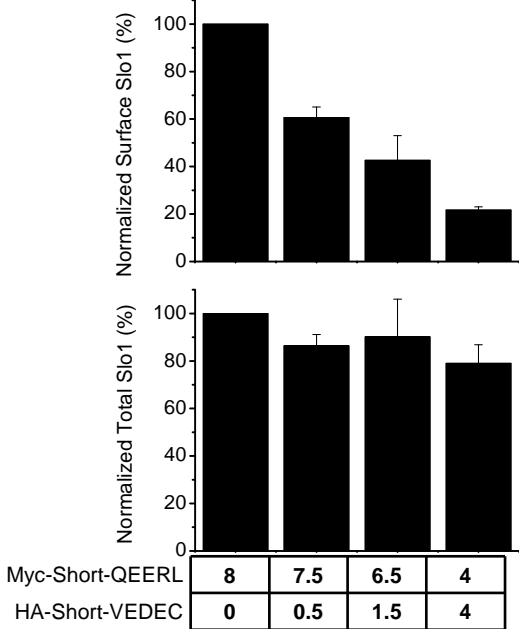


Fig. 7

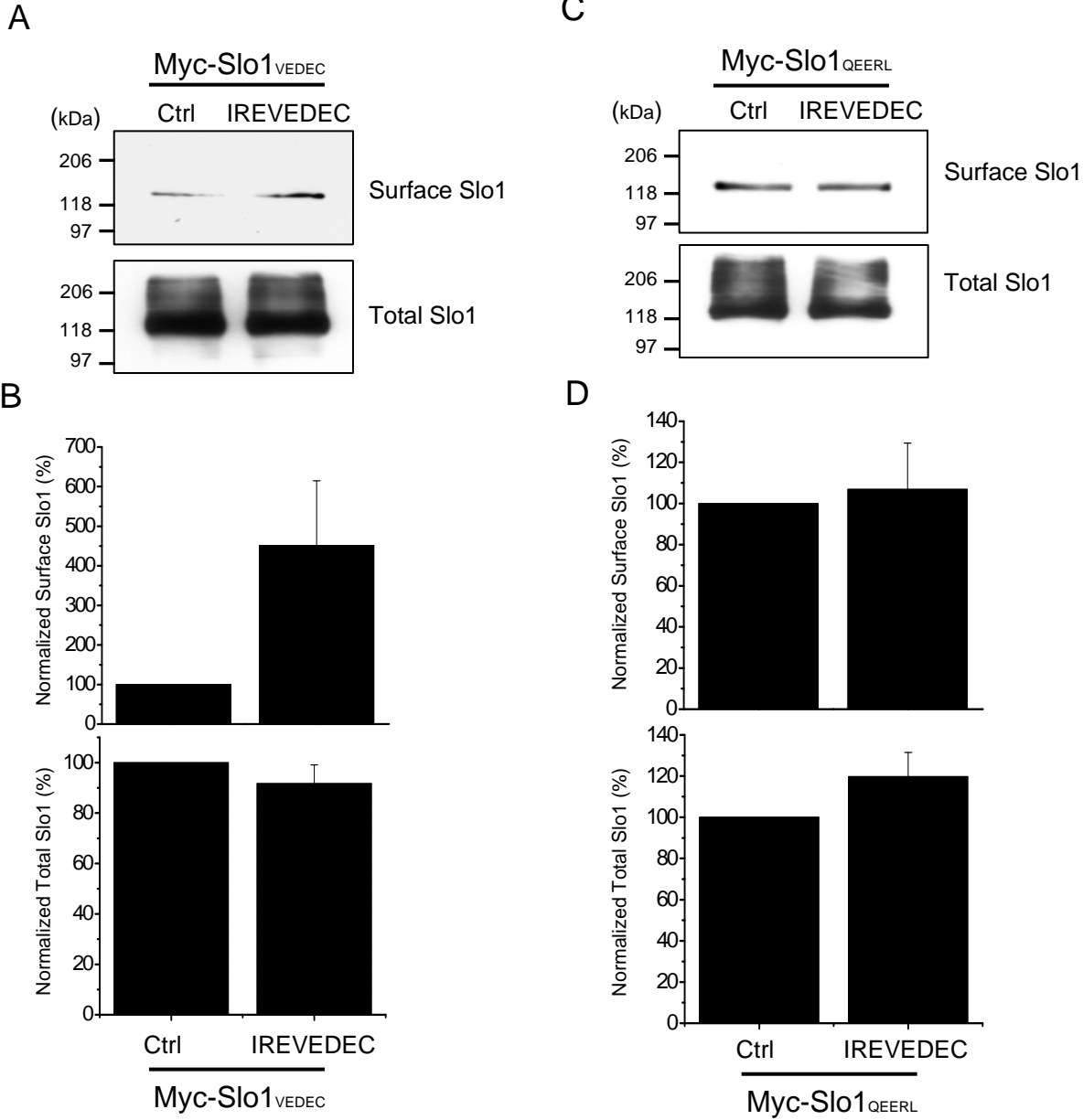


Fig. 8

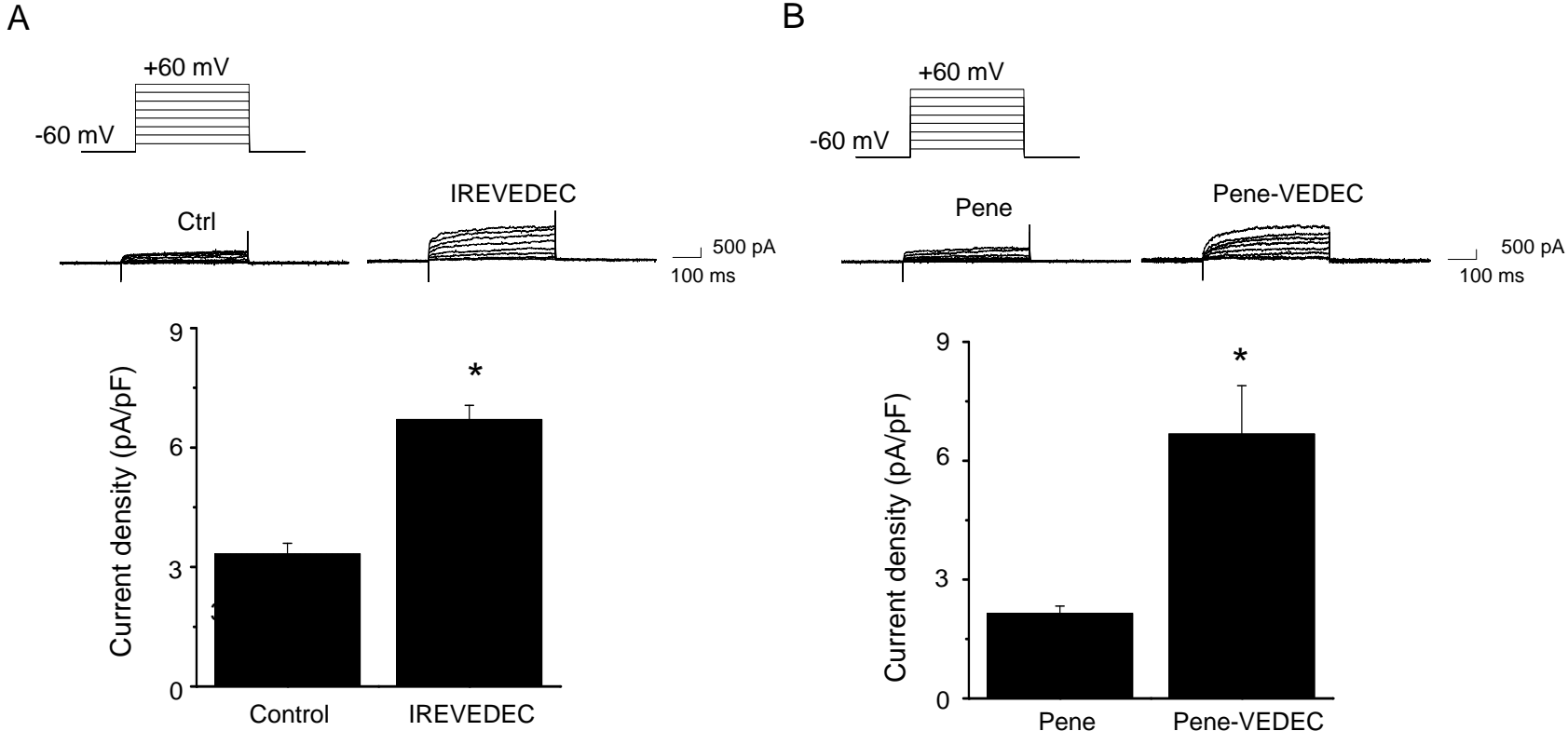


Fig. 9

